A Stochastic Model for Circadian Rhythms from Coupled Ultradian Oscillators

R. Edwards* R. Gibson
R. Illner*
Department of Mathematics and Statistics
University of Victoria
Victoria, BC V8W 3P4

V. Paetkau*
Department of Biochemistry and Microbiology
University of Victoria
Victoria, BC V8P 5C2

September 2, 2005

Abstract

A mechanism of coupled transcriptional-translational oscillators (TTOs) producing circadian oscillations as "beats" in individual cells is presented. The TTOs are described in two versions: 1) a version in which the activation or inhibition of gene sites is regulated stochastically, where the "free time" of the site under consideration depends on the concentration of a protein complex produced by another site, and 2) a deterministic, "time-averaged" version in which the switching between the "free" and "occupied" states of the sites occurs so rapidly that the stochastic effects average out. The second case is proved to emerge from the first in a mathematically rigorous way. Numerical results for both scenarios are presented and compared.

*Supported by grants from the Natural Science and Engineering Council of Canada

1 Introduction

We are concerned with molecular mechanisms that can account for circadian rhythms at the cellular level. Although circadian oscillators exist in complex multicellular organisms as well as in single-cell organisms, it is thought that most occur in single cells ([2], [8], [11]). We have previously [3] described a model for circadian oscillations in which ultradian oscillators, which have been widely observed to occur in cells, are coupled to produce circadian periods. The model was based, as is much of the related literature, on so-called transcriptional-translational oscillators (TTOs), in which genes are activated or inhibited for transcription by protein products of the oscillating system itself (transcriptional activators or suppressors, respectively). Several models for interactions between more than one oscillator to generate a circadian one have been described ([1], [13], [9]), but ours differs in positing coupling between the protein products of independent ultradian oscillators.

A challenging feature of TTOs is the fact that in cells, a given transcribed gene is present in one, or at most a small number of, copies, and its interaction with a transcriptional regulator is not correctly modeled by deterministic differential equations as used in [3]. Rather, because the number of copies of an expressed gene in a cell is zero, one, or possibly two, such interactions are more accurately described by stochastic equations, and this has been done for a number of existing models ([4], [13], [7]), using a classical algorithm due to Gillespie [6]. In some cases this results in shorter autocorrelation times [4] or random fluctuations [13]. Our objective here is to apply the stochastic approach to a model similar to the one described in [3], with particular reference to the apparent rates of binding of transcriptional regulatory proteins to their target sites. There is something of a paradox in these binding rates, as it has been observed that the rate is some 100-1000 times faster than the maximal diffusion-limited rate. In particular, a second-order rate constant $> 10^{10} M^{-1} s^{-1}$ has been experimentally measured for the association of the *E.coli* lac repressor with the lac operator site ([10],[15]). A detailed experimental and theoretical analysis ([14],[15]) has shown that the high rate of binding is due to low-specificity binding of the repressor to DNA, followed by rapid, one-dimensional diffusion to the specific binding site. Such a process allows for observed binding rates higher than the theoretical three-dimensional diffusion limit.

We have incorporated this rate, together with other parameters previously described, into a refined version of our coupled model, in which the DNA binding steps have been treated as stochastic processes. The subsequent step of translation of mRNA into protein has been left as a deterministic one, since the numbers of molecules in this process are larger. We

suggest that if the model is well-behaved with the critical DNA-binding step as a stochastic process, then the remaining steps can be left as deterministic without compromising the reliability of the model.

Three quite different time scales arise in the model. The binding and unbinding of the inhibiting (activating) protein complexes at the transciption sites occur on a very fast time scale, an aspect of our model motivated by the observations in [15] and alluded to in the previous paragraph. We introduce an (artificial) parameter ϵ of dimension time to adjust the time scales for these bindings and to explore the limit $\epsilon \to 0$. In the numerical tests in Section 4 we vary ϵ; in particular, for some of the simulations the value $\epsilon = 2.8 \times 10^{-5}\ hrs$ is used: this corresponds to an average of roughly 10 binding events per second. As shown in Section 4, this small value of ϵ produces results which, for all practical purposes, are indistinguishable from the simulations for a time-averaged deterministic model which is obtained in the limit $\epsilon \to 0$.

The second significant time scale is given by the periods of the individual ultradian oscillators, which are of the order of a few hours. The critical parameters for these oscillations are those describing the half-lives of mRNA, proteins, and protein complexes. In section 5 we conduct a brief exploratory analysis of the range of periods of our "primary" oscillators.

The third time scale is, of course, the circadian rhythm time scale, which in our model arises from a coupling of two of the simpler ultradian oscillators of slightly different frequencies. Natural selection could explain why pairs of frequencies leading to the right "beats" have emerged in the course of evolution. In fact, the common occurrence of ultradian oscillators would make it easy for evolution to produce circadian rhythms out of different components in different organisms, as is actually observed [3]. This mechanism has the added advantages of robustness and easy adaptability (the period of the beat will change with minor adjustments of the frequency ratio between the two primary oscillators). A power spectrum analysis demonstrates the robustness of the model with respect to the parameter ϵ.

2 The Model

Our model involves TTOs contained in a single cell. As described in [3], the model comprises two ultradian "primary" oscillators whose protein products are coupled to drive a circadian rhythm. For simplicity, the two coupled primary oscillators are essentially identical, with only their frequencies different, since the critical feature is the ability to couple TTOs through known molecular processes (formation of transcriptional-regulatory protein heterodimers).

Therefore, the key question regarding the ability of a stochastic process to describe stable circadian oscillators can be addressed in terms of one primary oscillator. In this system, two genes (DNA sites) are transcribed into mRNA, and this process is the origin of the following chemical dynamics.

- Transcription by gene 1 occurs when Site 1 (its regulatory region) is unoccupied. Its state is given by a random variable X_1, so that

  $X_1 = 0$ if site 1 is empty; $\quad X_1 = 1$ if site 1 is occupied by D_2 (see below)

- When gene 1 is active it produces mRNA (measured in molecules per cell, R_1) at a constant rate k_{13}. These molecules undergo first-order decay with a rate constant k_{14}.

- The mRNA molecules are translated into protein P_1, which either: (a) decays at rate k_{16}, (b) forms homodimers D_1 at rate k_{17}, or, (c) forms heterodimers D_{13} with proteins P_3 from a third gene (see below) with a rate constant k_{61}.

- The homodimer D_1 binds to site 2, and thereby activates the transciption of gene 2. The state of gene 2 is given by the value of a random variable Y_1 so that

  $Y_1 = 0$ if site 2 is empty, and $Y_1 = 1$ if site 2 is occupied by D_1.

- Transcription of gene 2 and translation of its mRNA into protein P_2 leads to formation of homodimer D_2, which feeds back to inhibit gene 1 (above).

- These linked reactions generate a TTO for an appropriate choice of parameters. The parameters used in our subsequent calculations are listed in Table 1. Our model entails gene 1 being inhibited by homodimer D_2 and gene 2 being activated by homodimer D_1. This is the mechanism leading to *primary* oscillations.

We denote by $R_i, P_i, D_i, \quad i = 1, 2$ the concentrations of the mRNA, the translated protein and the homodimer produced by site i. The above scenario is then summarized in the following system of stochastic differential equations. The parameters k_{13} etc. have the same meaning as in Ref. [3], and we have kept the notation used there; this explains the unconventional numbering (some of the equations from the reference, and hence some of the parameters, are no longer needed).

$$
\begin{aligned}
R_1' &= k_{13}(1 - X_1) - k_{14}R_1 && (1)\\
P_1' &= k_{15}R_1 - k_{16}P_1 - 2k_{17}P_1^2 + 2k_{18}D_1 - k_{61}P_1P_3 + k_{62}D_{13} && (2)\\
D_1' &= k_{17}P_1^2 - k_{18}D_1 && (3)\\
R_2' &= k_{13}Y_1 - k_{14}R_2 && (4)\\
P_2' &= k_{25}R_2 - k_{16}P_2 - 2k_{27}P_2^2 + 2k_{28}D_2 && (5)\\
D_2' &= k_{27}P_2^2 - k_{28}D_2 && (6)
\end{aligned}
$$

The last two terms in the second equation reflect the combination of proteins P_1 and P_3 (which is produced by the second primary oscillator) to form the heterodimer D_{13}. This heterodimer in turn breaks down into pairs P_1 and P_3 at rate k_{62}.

The second primary oscillator is given by a nearly identical set of equations, except that the periods of the oscillations are slightly different. This can, of course, be achieved by changing the parameters in many ways, but the simplest method is to have the two TTOs identical in nature but with different time scales. To do this we simply multiply each right hand side by a fixed constant $\delta > 0$, where δ is close (but not identical) to one. For example, the first equation of the second oscillator will read

$$R_3' = \delta(k_{13}(1 - X_2) - k_{14}R_3).$$

The parameters chosen reflect, where available, reasonable choices of known molecular processes. The critical ones for establishing the periods of the primary oscillators are the decay times of the mRNAs and proteins. For the former, a half-life of 13-17 minutes and for the latter, 4-17 minutes generate ultradian oscillations in the model. The values used in the simulation are given in Table 1.

The coupling between the two sites communicating in each oscillator is, of course, provided by the random variables X_i, Y_i. The times for which these random variables stay constant are assumed to be exponentially distributed. For example,

$$
\begin{aligned}
Prob\{X_1 = 0 \quad \text{in } (0,t) | X_1(0) = 0\} &= \exp(-D_2 t/\epsilon),\\
Prob\{X_1 = 1 \quad \text{in } (0,t) | X_1(0) = 1\} &= \exp(-rt/\epsilon)
\end{aligned}
$$

while

$$
\begin{aligned}
Prob\{Y_1 = 0 \quad \text{in } (0,t) | Y_1(0) = 0\} &= \exp(-D_1 t/\epsilon),\\
Prob\{Y_1 = 1 \quad \text{in } (0,t) | Y_1(0) = 1\} &= \exp(-st/\epsilon).
\end{aligned}
$$

Parameter	Value
k_{13}	1800
k_{14}	3.2
k_{15}	700
k_{16}	4
k_{17}	3.6×10^{-4}
k_{18}	15
k_{25}	1400
k_{27}	10^{-4}
k_{28}	5

Parameter	Value
k_{53}	500
k_{54}	0.8
k_{57}	6.8×10^{-4}
k_{58}	3
k_{61}	5×10^{-6}
k_{62}	0.3
r	25
s	5000
q	5500
δ	1.125

Table 1: Parameters per unit time (hrs.)

Here r and s are constants; ϵ is a time scaling parameter, introduced for convenience to exploit the fact that the binding and unbinding of the homodimers occurs on a faster time scale than the remaining processes. We use ϵ to properly gauge the most critical parameter, namely the rate constant for binding of the transcriptional-regulatory proteins (D_1, D_2) to the sites of the genes. Experimental work ([14], [10]) indicates macroscopic (observed) second-order binding rates of $10^{10}/(M \cdot \mathrm{s})$. In terms of molecules per cell in a bacterium, this translates into approximately $36,000$ molecules/(cell $\cdot$ hour) (1 molecule per bacterial cell is about 10^{-9} M).

The average "free" time of the binding site for D_2 is thus ϵ/D_2, and the average "occupied" time is ϵ/r. Their quotient is independent of ϵ, but will change with the homodimer concentration D_2. Similar interpretations apply for X_2 and Y_2 and the random variables associated with the second primary oscillator.

The average times for which a dimer stays bound $(\epsilon/r, \epsilon/s,$ etc.) are independent of the state of the system. In contrast, the "free" times are inversely proportional to the concentration of the attaching homodimer. In one of the simulations given in Section 4 we use $r = 25$ and $\epsilon = 10^{-1}$sec (which corresponds to $\frac{\epsilon}{r} = \frac{1}{250}$sec, or an average of 900,000 binding events per hour). We shall see that the corresponding stochastic simulation compares well with a limiting scenario for which $\epsilon = 0$. Before we describe this limiting scenario in detail we present the remaining equations making up the complete oscillatory system.

As stated earlier, the protein products P_1 and P_3 of the first and second primary oscillators combine to produce the heterodimer D_{13}. As formulated in the model, this heterodimer binds to the regulatory site of a fifth gene and

activates it for transcription (other constructs, involving other heterodimeric products of the two primary oscillators, and either stimulation or inhibition of transcription of the fifth gene, could also be used). Transcription, translation, and dimerization of the protein product of gene 5 yields the product D_5, which is the primary circadian output of the model (although all variables show circadian behaviour to a greater or less extent, as seen in the graphical results).

The corresponding system is

$$\begin{aligned} D_{13}' &= k_{61}P_1P_3 - k_{62}D_{13} && (7)\\ R_5' &= k_{53}X_3 - k_{54}R_5 && (8)\\ P_5' &= k_{15}R_5 - k_{16}P_5 - 2k_{57}P_5^2 + 2k_{58}D_5 && (9)\\ D_5' &= k_{57}P_5^2 - k_{58}D_5, && (10) \end{aligned}$$

and

$$Prob\{X_3 = 0 \text{ in } (0,t) | X_3(0) = 0\} = \exp\left(\frac{-D_{13}}{\epsilon}t\right),$$

$$Prob\{X_3 = 1 \text{ in } (0,t) | X_3(0) = 1\} = \exp\left(\frac{-q}{\epsilon}t\right).$$

3 The time-averaged deterministic model

We employ renewal reward theory (see [12]) to derive a system of ordinary differential equations which replaces (1-6) by a "time-averaged" system in the limit $\epsilon \to 0$. To this end, note first that if D_2 were independent of time, the time average of $X_1(t)$ over "macroscopic" time intervals (i.e., intervals of scale much larger than ϵ) is $\frac{D_2}{r+D_2}$. The corresponding average of $1 - X_1(t)$ is then $\frac{r}{r+D_2}$. Renewal reward theory implies that this intuition is mathematically accurate.

Specifically, define a cycle to consist of a period of unoccupied time followed by a period of occupied time. The cycle ends with detachment. The period of unoccupied time is exponentially distributed with mean ϵ/D_2. Suppose, in the language of renewal reward theory, that no reward is received during this time. The following occupied part of the cycle is exponentially distributed with mean ϵ/r, and we assume that the reward associated with this period is exactly equal to the amount of occupied time. Then, by renewal reward theory, the long-term average reward (i.e., the proportion of occupied time) is with probability 1 equal to $E(R)/E(L)$ where $E(R)$ is the

expected reward during a cycle and $E(L)$ is the expected length of a cycle. In the case under consideration

$$E(R) = \epsilon/r, \quad E(L) = \epsilon/r + \epsilon/D_2,$$

so the long-term time average of $X_1(t)$ is $D_2/(r + D_2)$, i.e., $\lim_{\epsilon\to 0} X_{1\epsilon}(t) = \frac{D_2}{r+D_2}$ (here, we denote the random variables X_i as $X_{i\epsilon}$ to emphasize the dependence on ϵ). This time average will hold over any time interval over which D_2 is constant or changes sufficiently slowly. In this time-averaged system Eqns. (1,4) then become

$$R_1' = k_{13}\frac{r}{r + D_2} - k_{14}R_1 \tag{11}$$

$$R_2' = k_{13}\frac{D_1}{s + D_1} - k_{14}R_2 \tag{12}$$

and the remaining equations stay the same. Similarly, Equation (8) becomes

$$R_5' = k_{53}\frac{D_{13}}{(q + D_{13})} - k_{54}R_5.$$

This intuitive argument is not rigorous. As is transparent from the equations for the primary oscillators, all the dependent variables are random variables with time fluctuations at time scale ϵ. In particular, D_1 and D_2 (and likewise D_3 and D_4) experience stochastic fluctuations in their third derivatives (R_1' experiences random jumps, as does P_1'', and as does D_1'''). The integration process involved in the computation of D_i, $(i = 1, 2)$ will average out these fluctuations, so that D_i will indeed vary more slowly than, say, R_i. An argument based on the Arzelà-Ascoli Theorem can be used to translate these observations into a mathematical proof.

To this end we denote by $R_{1\epsilon}, P_{1\epsilon}, D_{1\epsilon}$ etc. the solution of (1-6) for some $\epsilon > 0$ and given initial values $R_1(0), P_1(0), \ldots$, and denote by R_1, P_1, D_1 etc. the solution of Eqns. (11, 12) ff. for the same initial values. We prove

Proposition 1. *Almost surely for all $t > 0$,*

$$\lim_{\epsilon\to 0} R_{1\epsilon}(t) = R_1(t)$$

$$\lim_{\epsilon\to 0} P_{1\epsilon}(t) = P_1(t)$$

$$\lim_{\epsilon\to 0} D_{1\epsilon}(t) = D_1(t)$$

$$\lim_{\epsilon\to 0} R_{2\epsilon}(t) = R_2(t)$$

etc.

Proof.

Step 1. Consider an arbitrary but fixed time interval $[0, T]$ and let (ϵ_n) be a sequence such that $\epsilon_n \to 0$ as $n \to \infty$. For each n we consider a realization, again denoted by $R_{1\epsilon}$ etc., of the initial value problem (1-6) ff. with the given fixed initial data.

The resulting functions $R_{1\epsilon_n}, P_{1\epsilon_n}, D_{1\epsilon_n}, \ldots$ all remain bounded and have (uniformly in ϵ) bounded first derivatives on $[0, T]$. By the Arzelà-Ascoli Theorem, there is a convergent subsequence of ϵ_n, denoted again by ϵ_n. We denote the limits by $\tilde{R}_1, \tilde{P}_1, \ldots$. What we show next is that these limits are solutions of the deterministic limit equations (11,12) ff.

Step 2. We write ϵ rather than ϵ_n to simplify the notation. Observe that

$$R_{1\epsilon}(t) = R_1(0)e^{-k_{14}t} + k_{13}\int_0^t (1 - X_{1\epsilon})(\tau)e^{k_{14}(\tau - t)}\, d\tau$$

and

$$R_1(t) = R_1(0)e^{-k_{14}t} + k_{13}\int_0^t \frac{r}{r + D_2(\tau)}e^{k_{14}(\tau - t)}\, d\tau.$$

The central step of our proof is showing that $\tilde{R}_1$ and $\tilde{D}_2$ are also related by (11). This will follow if we can show that for any differentiable function $f = f(\tau)$ and any fixed time interval $[s, t]$

$$\lim_{\epsilon \to 0} \int_s^t (1 - X_{1\epsilon})(\tau)f(\tau)\, d\tau = \int_s^t \frac{r}{r + \tilde{D}_2(\tau)} f(\tau)\, d\tau.$$

To this end consider a partition $\{s, s + \Delta, s + 2\Delta, \ldots, s + n\Delta = t\}$ of $[s, t]$, where $\Delta = \frac{t-s}{n}$. Then

$$\int_s^t (1 - X_{1\epsilon})(\tau)f(\tau)\, d\tau = \sum_{k=0}^{n-1} \int_{s+k\Delta}^{s+(k+1)\Delta} (1 - X_{1\epsilon})(\tau)f(\tau)\, d\tau.$$

On $[s + k\Delta, s + (k + 1)\Delta]$ we have

$$f(\tau) = f(s + k\Delta) + O(\Delta)$$

so

$$\int_{s+k\Delta}^{s+(k+1)\Delta} (1 - X_{1\epsilon})(\tau)f(\tau)\, d\tau = [f(s + k\Delta) + O(\Delta)] \int_{s+k\Delta}^{s+(k+1)\Delta} (1 - X_{1\epsilon})(\tau)\, d\tau$$

Because of the equicontinuity we have uniformly in ϵ

$$D_{2,\epsilon}(\tau) = \tilde{D}_2(s + k\Delta) + O(\Delta) + \mu(\epsilon),$$

where $\mu(\epsilon) \to 0$ as $\epsilon \to 0$. Hence, by the renewal reward result quoted earlier [12]

$$\lim_{\epsilon \to 0} \int_{s+k\Delta}^{s+(k+1)\Delta} (1 - X_{1\epsilon})(\tau) f(\tau)\, d\tau = \frac{r\Delta}{r + \tilde{D}_2(s + k\Delta) + O(\Delta)} f(s + k\Delta) + O(\Delta^2)$$

so

$$\lim_{\epsilon \to 0} \int_s^t (1 - X_{1\epsilon})(\tau) f(\tau)\, d\tau = \sum_{k=0}^{n-1} \frac{r}{r + \tilde{D}_2(s + k\Delta)} \Delta f(s + k\Delta) + O(\Delta),$$

and in the limit $\Delta \to 0$ the right hand side converges to

$$\int_s^t \frac{r}{r + \tilde{D}_2(\tau)} f(\tau)\, d\tau.$$

Step 3. The argument in step 2 and similar (but simpler) reasonings for the other dependent variables show that the R_i, P_i and $D_i, i = 1, 2$ and the $\tilde{R}_i, \tilde{P}_i$ and $\tilde{D}_i$ are both solutions of the same initial value problem. By unique solvability it follows that these solutions are identical, so for example $\tilde{R}_1(t) = R_1(t)$ for all t. This uniqueness also implies (by a standard argument) that the passage to a subsequence of the ϵ_n made earlier is not necessary, but that in fact $\lim_{\epsilon \to 0} R_{i\epsilon}(t) = R_i(t)$, and likewise for all other dependent variables.

This completes the proof.

4 Numerical tests

Here we present some results of simulations performed with the XPPAUT package (see [5], or http://www.math.pitt.edu/ ~bard/xpp/xpp.html). The chosen parameters are those from Table 1. Figure 1 shows the time course of the proteins P_1 and P_3 for the deterministic model, which oscillate with a period of about 3 hours but differ slightly in their periods. A slight circadian variation is seen; it is much more promiment in Figure 2, where the responses of the protein products of the fifth DNA site are shown; note the time lag of D_5 with respect to D_{13}.

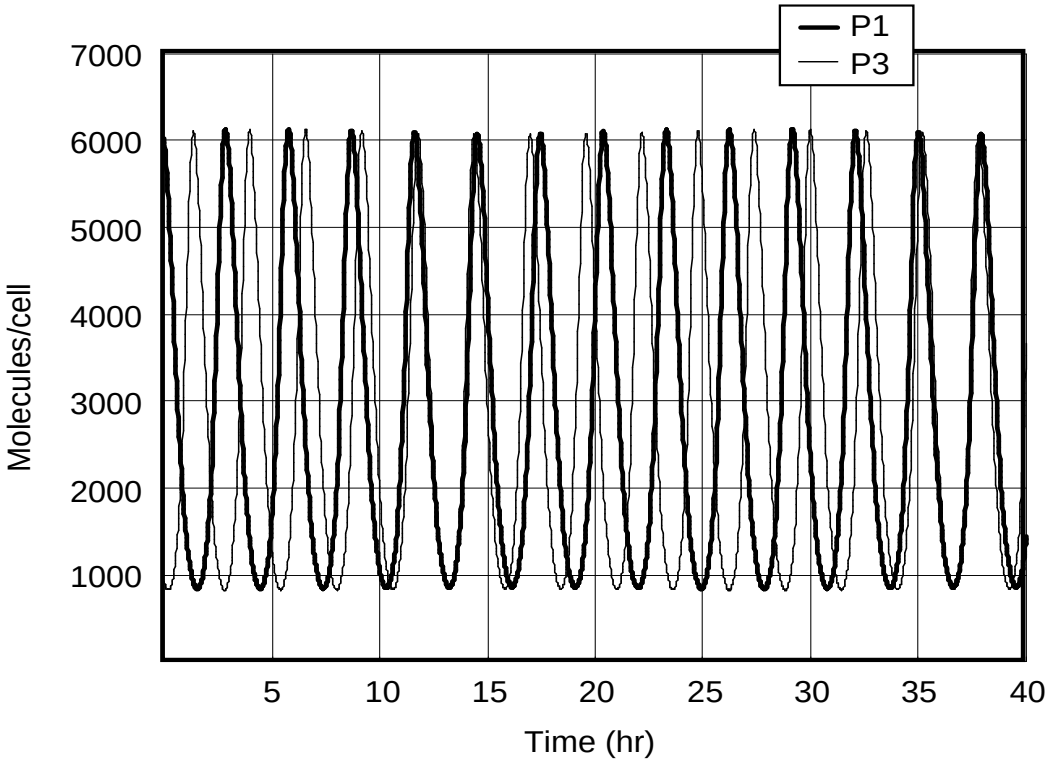

Figure 1: The time evolution of the proteins P_1 and P_3 according to the time-averaged model

In Figures 3 and 4 the same calculation was done for the stochastic model. This calculation used Gillespie's method [6], where the ϵ was chosen as $2.8 \times 10^{-5} hrs$. The results are essentially identical to the ones for the time-averaged model.

As a control measure we performed some calculations with larger ϵ, for example $\epsilon = 2.8 \times 10^{-3}$ hrs and $\epsilon = 0.028$ hrs. For the former case, especially, the results were close to the time-averaged simulations. For the latter case, deviations from the time-averaged simulations became noticable: the amplitude of the circadian oscillations in D_5 fluctuated stochastically and their period decreased slightly.

Despite these more significant stochastic effects with larger ϵ, the integrity of the circadian period is remarkably robust in our model with respect to the choice of ϵ. We demonstrate this by computing Fourier power spectra of D_5 time series generated by simulations with $\epsilon = 2.8 \times 10^{-5}$ and $\epsilon = 2.8 \times 10^{-2}$ (see Figures 5 and 6). The former was calculated from a time series of 7447 data points at intervals of 1 minute, representing 124.1 hours of real time. The latter was calculated from a time series of 9920 data points at

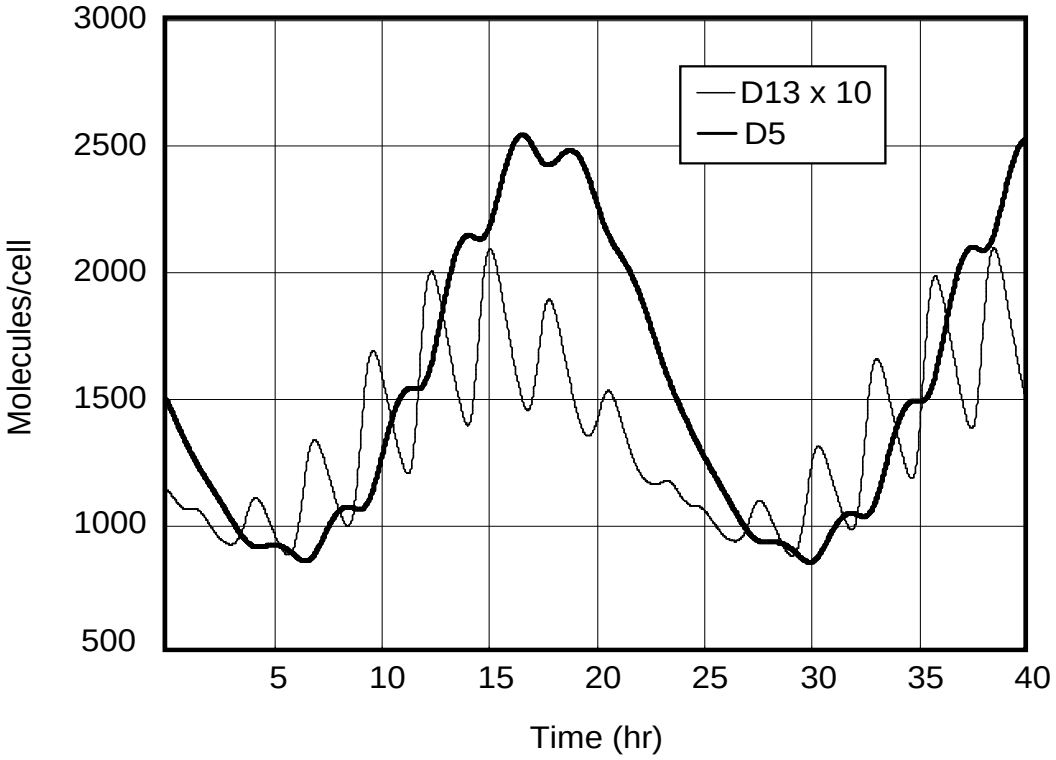

Figure 2: The time evolution of the heterodimer D_{13} and the homodimer D_5 according to the time-averaged model

intervals of 10 minutes, representing 1653.2 hours of real time. We chose to integrate for a longer time in the latter case because the circadian oscillations were less regular. The power spectrum is shown in decibels (decibels = $10\log_{10}$(power), where power $= |X_i|^2$ for X_i, the i^{th} frequency component of the Fourier transform of the time series $\{x_k\}$). The frequencies of the primary oscillators show up clearly in the power spectra at close to 8 and 9 cycles per day respectively, and the circadian oscillations are clearly overwhelmingly dominant at close to (but not exactly) 1 cycle per day in both cases. Even after 65 "days" with $\epsilon = 0.028$, the stochastic oscillator remained in phase with the circadian period; the wave form appeared to persist indefinitely.

5 Remarks on the frequencies of the primary oscillators

The fundamental idea of our model is that circadian oscillations can easily be achieved via coupling of faster oscillators. We now address the question of

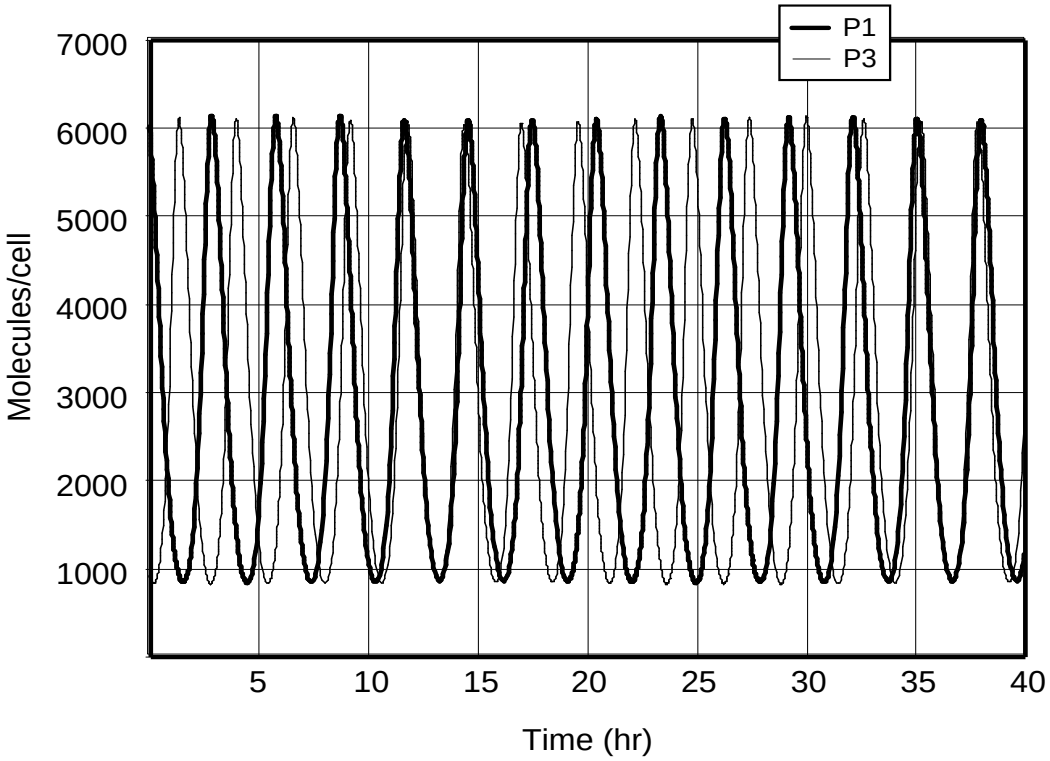

Figure 3: The time evolution of the proteins P_1 and P_3 according to the stochastic model

whether the primary oscillators could attain circadian periods without need for coupling within reasonable ranges of parameter values based on known biochemistry. To this end we investigated which (if any) intrinsic limitations there are on the periods of the primary oscillators introduced earlier. We first explored (randomly) variations of the growth parameters k_{13}, k_{15}, k_{17}, etc., and the unbinding rates r and s to see how they would affect the periods of the time-averaged single primary oscillator

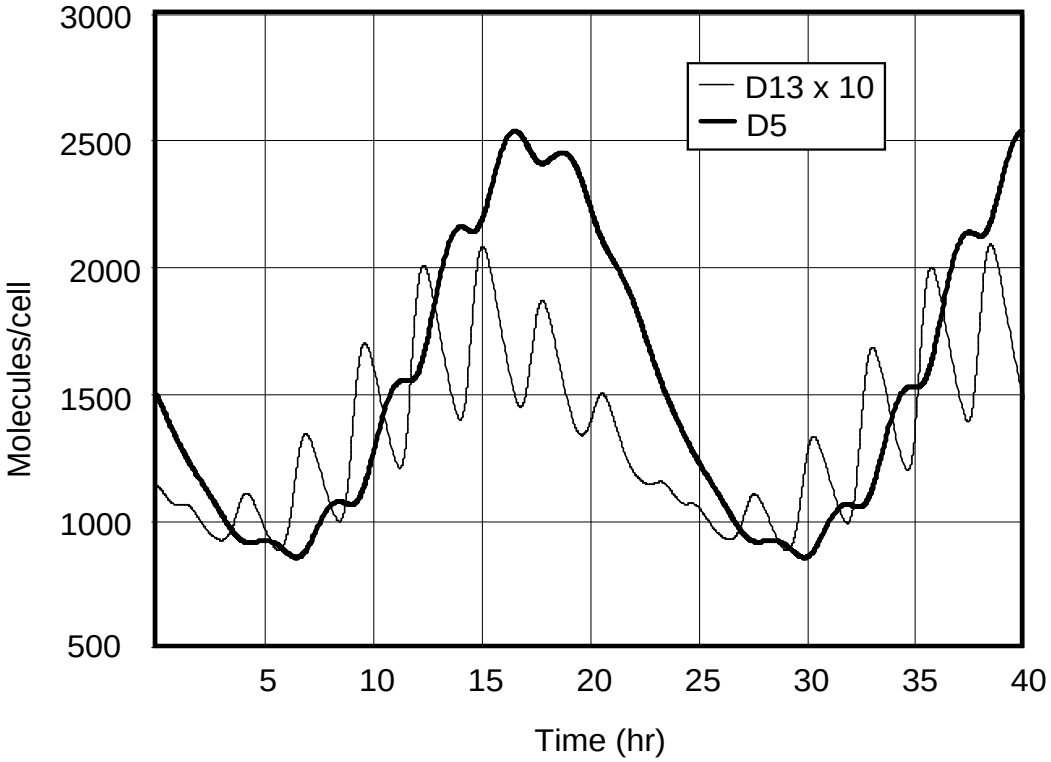

Figure 4: The time evolution of the heterodimer D_{13} and the homodimer D_5 according to the stochastic model

$$\begin{aligned}
\frac{dR_1}{dt} &= k_{13}\frac{r}{r+D_2} - k_{14}R_1 \\
\frac{dP_1}{dt} &= k_{15}R_1 - k_{16}P_1 - 2k_{17}P_1^2 + 2k_{18}D_1 \\
\frac{dD_1}{dt} &= k_{17}P_1^2 - k_{18}D_1 \\
\frac{dR_2}{dt} &= k_{13}\frac{D_1}{s+D_1} - k_{14}R_2 \\
\frac{dP_2}{dt} &= k_{25}R_2 - k_{16}P_2 - 2k_{27}P_2^2 + 2k_{28}D_2 \\
\frac{dD_2}{dt} &= k_{27}P_2^2 - k_{28}D_2
\end{aligned} \tag{13}$$

Initially we kept the decay parameters k_{14}, k_{16}, k_{18} fixed and just varied k_{13}. This had a modest effect on the period; the longest which was observed

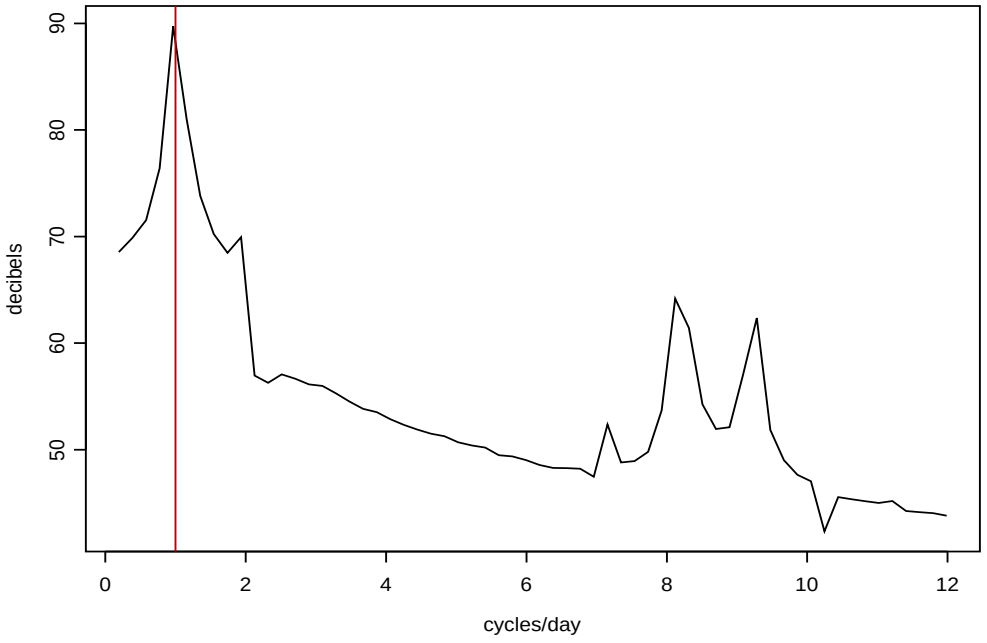

Figure 5: Power spectra for D_5 when $\epsilon = 2.8 \times 10^{-5}$ (no smoothing)

was 3.5 hrs. Random experiments of this nature did not produce periods of circadian length.

For a systematic investigation of the dependence of the periods on the parameters, we then set $k_{25} = k_{15}, k_{27} = k_{17}, k_{28} = k_{18}$ and linearized the system about its unique positive equilibrium $(R_{1E}, P_{1E}, D_{1E}, R_{2E}, P_{2E}, D_{2E})$. The linearization yields the 6-by-6 matrix

$$A = \begin{pmatrix} -k_{14} & 0 & 0 & 0 & 0 & \frac{-k_{13}r}{(r+D_{2E})^2} \\ k_{15} & -k_{16} - 2k_{17}P_{1E} & 2k_{18} & 0 & 0 & 0 \\ 0 & 2k_{17}P_{1E} & -k_{18} & 0 & 0 & 0 \\ 0 & 0 & \frac{k_{13}s}{(s+D_{1E})^2} & -k_{14} & 0 & 0 \\ 0 & 0 & 0 & k_{15} & -k_{16} - 2k_{17}P_{2E} & 2k_{18} \\ 0 & 0 & 0 & 0 & 2k_{17}P_{2E} & -k_{18} \end{pmatrix}$$

Its eigenvalues satisfy $\det(A - \lambda I) = 0$. This yields the characteristic equation

$$(k_{14} + \lambda)^2(k_{18} + \lambda)^2(k_{16} + 2k_{17}P_{1E} + \lambda)(k_{16} + 2k_{17}P_{2E} + \lambda) + c_0^2 \ = 0.$$

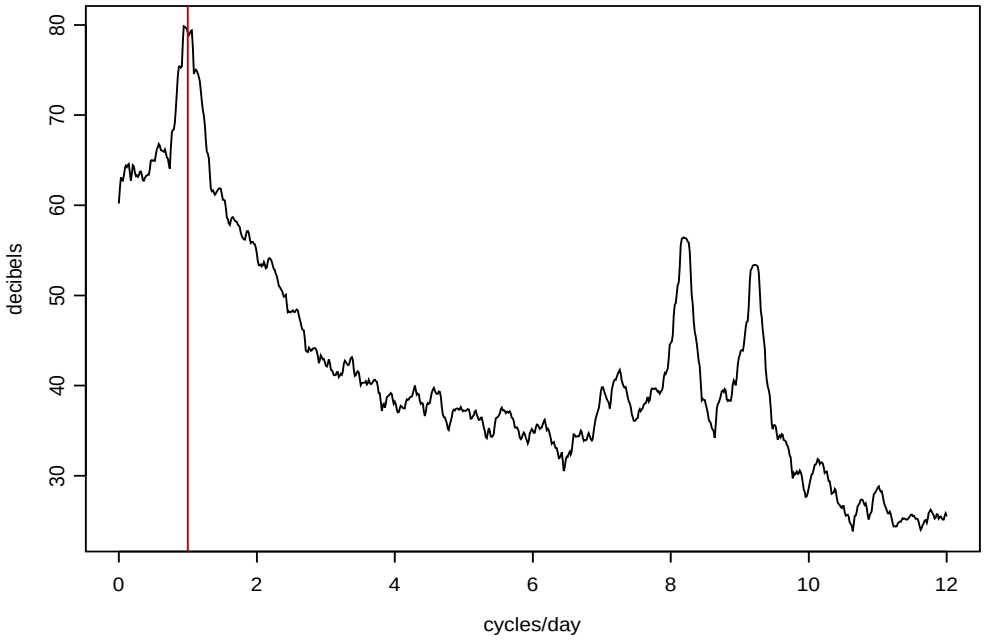

Figure 6: Power spectra for D_5 when $\epsilon = 2.8 \times 10^{-2}$ (smoothed with a Daniell filter of length 11).

Here,

$$c_0^2 = \frac{4k_{15}^2 k_{17}^2 k_{13}^2 rs}{(s + D_{1E})^2 (r + D_{2E})^2}.$$

To identify solutions with longer periods we look for a pair of eigenvalues with positive real part and small imaginary parts. Observe that $c_0^2 = 0$ in (5) produces 6 real and negative eigenvalues (eigenvalues are counted with their multiplicity). If we now increase c_0^2, one pair of eigenvalues approaches and eventually crosses the imaginary axis (Hopf bifurcation), producing the oscillations. However, the only way to force the crossing of the imaginary axis at small imaginary value is to move a pair of eigenvalues closer to the imaginary axis to begin with (i.e., when $c_0^2 = 0$).

To achieve this, we first modified the parameter k_{17} governing the rate of homodimer formation. However, decreasing k_{17} turns out to increase P_{1E}, counter-acting attempts to move the crossing pair closer to the real axis.

Finally, the actual rate of homodimer decay, k_{18}, is not known, although it is unlikely to be smaller than 1 per hour. Choosing it to be exactly 1

per hour (earlier it was set to 15 per hour) we increased the periods up to 9 hours. Setting k_{18} this low is probably not reasonable, but given no *a priori* firm bounds as to how small k_{18} can actually be (a comment that applies to k_{14} and k_{16} as well), no simple predictions on the size of the periods of the primary oscillators can be made.

The following set of parameters produces a wavelength of about 22 hours: $k_{13} = 1000,\ k_{14} = k_{16} = 1,\ k_{15} = 400,\ k_{17} = 10^{-5},\ k_{18} = 0.25,\ r = 1,\ s = 9000$. Thus almost circadian periods can be obtained, but only by stretching parameters beyond biochemically reasonable values.

6 Conclusions

We have shown that TTOs in both their stochastic and time-averaged versions produce stable ultradian oscillations for reasonable parameter choices. These oscillations are robust with respect to the scaling parameter governing the dimer-driven stochastic activation or inhibition of the relevant gene sites. Couplings of such TTOs with slight variations in their periods offer a simple mechanism to explain the emergence of circadian rhythms as "beats". This explanation has the added desirable feature of making circadian rhythms readily adaptable to evolutionary pressures.

References

[1] N. Barkai, S. Leibler (2000). *Circadian clocks limited by noise.* Nature **403**, 267-268

[2] J.C. Dunlap (1999). *Molecular bases for circadian clocks.* Cell **96**, 271-290

[3] R. Edwards, R. Illner, and V. Paetkau, Generation of Circadian rhythm by coupled ultradian oscillators, preprint at http://web.uvic.ca/sciweb/Papers/PapersIndex.htm

[4] M.B. Elowitz, S. Leibler (2000). *A synthetic oscillatory network of transciptional regulators.* Nature **403**, 335-338

[5] B. Ermentrout (2002). *Simulating, analyzing, and animating dynamical systems. A guide to XPPAUT for researchers and students.* SIAM Publ.

[6] D.T. Gillespie (1977). *Exact stochastic simulation of coupled chemical-reactions.* J. Phys. Chem. **81**, 2340-2361

[7] D. Gonze, J. Halloy, J.C. Leloup, and A. Goldbeter (2003). *Stochastic models for circadian rhythms: effect of molecular noise on periodic and chapotic behaviour.* C.R. Biol **326**, 189-203

[8] I. Mihalcescu, W. Hsing, and S. Leibler (2004). *Resilient circadian oscillator revealed in individual cyanobacteria.* Nature **430**, 81-85

[9] J.C. Leloup, A. Goldbeter (2003). *Toward a detailed computational model for the mammalian circadian clock.* Proc. Natl. Acad. Sci. USA **100**, 7051-7056

[10] A.D. Riggs, S. Bourgeois, and M. Cohn (1970). *The lac repressor-operator interaction. 3. Kinetic studies.* J. Mol. Biol. **53**, 401-417

[11] U. Schibler, F. Naef (2005). *Cellular oscillators: rhythmic gene expression and metabolism.* Curr. Opin. Cell Biol. **53**, 401-417

[12] S.M. Ross (1989). *Introduction to Probability Models.* 4th Ed., Academic Press

[13] J.M. Vilar, H.Y. Kueh, N. Barkai, and S. Leibler (2002). *Mechanisms of noise-resistance in genetic oscillators.* Proc. Natl. Acad. Sci. USA **99**, 5988-5992

[14] O.G. Berg, R.B. Winter, and P.H. von Hippel (1981). *Diffusion-driven mechanisms of protein translocation on nucelic acids. 1. Models and theory.* Biochemistry **20**, 6929-6948

[15] R.B. Winter, O.G. Berg, and P.H. von Hippel (1981). *Diffusion-driven mechanisms of protein-translocation on nucleic acids. 3. The Escherichia coli lac repressor-operator intercation: kinetic measurements and conclusions.* Biochemistry **20**, 6961-6977